Physiological Reports

Open Access

Physiological Reports ISSN 2051-817X

ORIGINAL RESEARCH

Novel description of the large conductance Ca^{2+}-modulated K^+ channel current, BK, during an action potential from suprachiasmatic nucleus neurons

John R. Clay

National Institute of Neurological Disorders and Stroke, National Institutes of Health, Bethesda, Maryland

Keywords
Action potential clamp, BK channels, mathematical models, suprachiasmatic nucleus neurons.

Correspondence
John R. Clay, Twinbrook 4S-26, 5625 Fishers Lane, Rockville, MD 20852.
Tel: 301-496-7711
E-mail: jrclay@ninds.nih.gov

Funding Information
This research was supported by the Intramural Research Program of the National Institute of Neurological Disorders and Stroke, National Institutes of Health, Bethesda, MD.

Received: 31 August 2017; Accepted: 19 September 2017

doi: 10.14814/phy2.13473

Physiol Rep, 5 (20), 2017, e13473, https://doi.org/10.14814/phy2.13473

Abstract

The contribution of the large conductance, Ca^{2+}-modulated, voltage-gated K^+ channel current, I_{BK}, to the total current during an action potential (AP) from suprachiasmatic nucleus (SCN) neurons is described using a novel computational approach. An experimental recording of an SCN AP and the corresponding AP-clamp recording of I_{BK} from the literature were both digitized. The AP data set was applied computationally to a kinetic model of I_{BK} that was based on results from a clone of the BK channel α subunit heterologously expressed in *Xenopus* oocytes. The I_{BK} model result during an AP was compared with the AP-clamp recording of I_{BK}. The comparison suggests that a change in the intracellular Ca^{2+} concentration does not have an immediate effect on BK channel kinetics. Rather, a delay of a few milliseconds may occur prior to the full effect of a change in Ca_i^{2+}. As shown elsewhere, the $\beta 2$ subunit of the BK channel in the SCN, which is present in the daytime along with the α subunit, shifts the BK channel activation curve leftward on the voltage axis relative to the activation curve of BK channels comprised of the α subunit alone. That shift may underlie the diurnal changes in electrical activity that occur in the SCN and it may also enhance the delay in the effect of a change in Ca_i^{2+} on BK kinetics reported here. The implication of these results for models of the AP for neurons in which BK channels are present is that an additional time dependent process may be required in the models, a process that describes the time dependence of the development of a change in the intracellular Ca^{2+} concentration on BK channel gating.

Introduction

BK channels are a significant factor underlying membrane excitability of suprachiasmatic nucleus (SCN) neurons (Cloues and Sather 2003; Jackson et al. 2004; Colwell 2006; Meredith et al. 2006; Pitts et al. 2006; Kent and Meredith 2008; Belle et al. 2009; Montgomery and Meredith 2012; Montgomery et al. 2013; Whitt et al. 2016). Specifically, they have been implicated in the diurnal changes in spontaneous firing that occur in the SCN (Colwell 2006; Meredith et al. 2006; Whitt et al. 2016). SCN neurons fire spontaneously at rates of 8-10 Hz during the day (Jackson et al. 2004). At night, the activity is suppressed typically to <2 Hz with many cells in the silent state (Inouye and Kawamura 1979; Green and Gillette 1982; Groos and Hendriks 1982; Shibata et al. 1982; Yamazaki et al. 1998). These neurons express a subunit, $\beta 2$, having the potential to modify BK channel properties (Montgomery and Meredith 2012; Whitt et al. 2016). The $\beta 2$ subunit produces inactivation of BK (Wallner et al. 1999; Xia et al. 1999). Inactivating BK currents are referred to as BK_i. BK currents that exhibit relatively little inactivation are referred to as BK_s. The primary BK component in the SCN during the day is BK_i, whereas BK_s is

the primary BK current in the SCN at night (Whitt et al. 2016). The latter group has suggested that the difference in the inactivation properties of these two BK channel types underlies the differences in excitability in SCN neurons between night and day; repetitive firing during the day (BK_i), versus relative quiescence at night (BK_s).

The focus of this report is on the contribution of BK_i channel current, I_{BK}, to the total current during an action potential (AP) in the daytime. Those results have been measured in SCN neurons using the AP-clamp technique (Jackson et al. 2004; Whitt et al. 2016), a method in which a previously recorded AP is applied to a neuron before and after addition to the external medium of a specific ion channel blocker (Llinas et al. 1982; Bean 2007). For example, the rapidly activating and inactivating sodium ion current, I_{Na}, has been measured in SCN neurons using the AP clamp together with tetrodotoxin, a specific blocker of I_{Na} (Jackson et al. 2004). The amplitude and time course of I_{Na} during an SCN AP was determined from the difference between the test and control results of the experiment. Jackson et al. (2004) also reported voltage clamp step recordings of I_{Na}, the traditional method for analyzing an ionic current (Hodgkin and Huxley 1952). The two approaches together provide a more complete description of a particular ion current component than is provided by voltage clamp step results alone. Jackson et al. (2004) reported a similar analysis for the calcium ion current, I_{Ca}. The I_{Ca} component is required for BK channel activation during an AP. In a recent study the I_{Na} and I_{Ca} results from Jackson et al. (2004) were analyzed computationally to obtain models of these components suitable for SCN neurons (Clay 2015). In this report that analysis has been extended to I_{BK}. The long-term goal of this work is a mathematical model of the AP for SCN neurons.

Methods

The results described below require an AP from an SCN neuron, the corresponding AP-clamp measurement of I_{BK}, both of which are provided by Jackson et al. (2004; their Fig 12 with I_{BK} corresponding to I_{KCa}), and a kinetic model of I_{BK} gating. The AP and I_{BK} recordings were digitized (Clay 2015). Those records are shown in Figure 1 with lines connecting the points. Figure 1 also contains simulations of I_{BK} at various points during the AP. The data sets V_i vs. t_i for the AP and $I_{BK,i}$ vs. t_i with $i = 0,1,2,\ldots$, are the basis for the analysis that follows with V membrane potential in millivolts, time t in milliseconds, and I_{BK} in picoamperes. The V_i vs. t_i data set for the AP was applied computationally to the model of I_{BK} given below using Mathematica (Wolfram Research, Champaign, IL; Clay 2015). That model is based on voltage clamp step recordings of Cui et al. (1997) from *mslo*, a clone of the BK channel α subunit heterologously expressed in *Xenopus* oocytes. Those results were obtained using the inside-out voltage clamp mode so that Ca_i^{2+} could be controlled during the experiments. A novel feature of the I_{BK} model concerns a putative Ca_i^{2+} dependence of some of its parameters. The model is given by:

$$I_{BK}(V,t) = g_{BK} n(V,t)(V - E_K) \quad (1)$$

where g_{BK} is BK channel conductance, g_{BK} = 38.5 nS, $n(V,t)$ is the voltage- and time-dependent gating variable of the channel, and E_K is the K^+ reversal potential, E_K = −96 mV (Jackson et al. 2004). The gating variable is determined by:

$$dn(V,t)/dt = -[\alpha_{BK}(V) + \beta_{BK}(V)]n(t) + \alpha_{BK}(V) \quad (2)$$

with

$$\alpha_{BK}(V) = -\alpha_{Ca}(V - V_{Ca})/\{\exp[-0.045(V - V_{Ca})] - 1\}\text{msec}^{-1}$$

$$\beta_{BK}(V) = \beta_{Ca}\exp[-(V - V_{Ca})/30]\text{msec}^{-1} \quad (3)$$

The various parameters of the model were determined by comparing its predictions with the recordings of Cui et al. (1997). The model in Equations 1–3 is similar to the one used by Hodgkin and Huxley (1952) for their analysis of I_K in squid giant axons with a Ca_i^{2+} dependence assigned to the model via V_{Ca}, α_{Ca}, and β_{Ca}

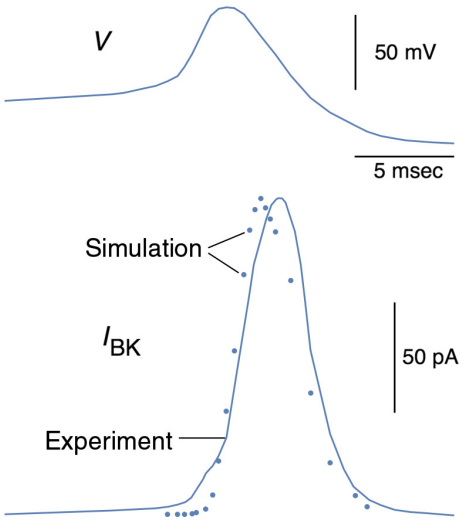

Figure 1. Top panel: AP from figure 12 of Jackson et al. (2004). The 0 mV level corresponds to the top of the bar labeled 50 mV. This waveform was used to obtain the AP-clamp recording of I_{BK} shown in the bottom panel along with a simulation of that result (filled circles), as described in the text.

(Equation 3; Results). The V_i vs. t_i data set of the AP in Figure 1 was applied to Equation 2 using a procedure described in Clay (2015) to determine BK channel activation throughout the AP. The start point of the AP in Figure 1 is $t_0 = 0$, $V_0 = -58$ mV. This level of V is below activation of I_{BK} during the interspike interval since Ca_i^{2+} during that time is ~50 nmol/L, the level of Ca_i^{2+} in a resting neuron (McCormick and Huguenard 1992). At this level of Ca_i^{2+}, $V = -58$ mV is below the activation range of I_{BK} (Cui et al. 1997; Xia et al. 1999), and so the start value for n, n_0, is assumed to be 0. The next iterative value of n, n_1, was determined from Equation 2 with NDSolve (Mathematica), using $V(t) = V_0 + (V_1-V_0)(t-t_0)/(t_1-t_0)$ for $t_0 < t < t_1$ ($V_1 = -53.5$; $t_1 = 5.6$ msec). The iterative values of Ca_i^{2+} were obtained as described in Clay (2015) and shown below (Results). This procedure was continued throughout the V_i versus t_i data set of the AP waveform. The resulting digitized values of I_{BK} corresponding to Equation 1 are $I_{BK,i} = g_{BK}\ n_i(V_i\text{-}E_K)$. Those results are shown in Figure 1 along with the experimental recording of I_{BK}. The model for I_{BK} does not contain an inactivation parameter since the results of Cui et al. (1997) do not clearly show inactivation over the duration of the voltage clamp steps - 20 msec - used for those results (Discussion).

Results

Cai^{2+} during an AP

As noted above, the intracellular calcium ion concentration, Ca_i^{2+}, during an AP from SCN neurons is required to determine I_{BK}. A model of I_{Ca} is, in turn, required for this result. This component cannot be described by $I_{Ca} = g_{Ca}(V\text{-}E_{Ca})$, where g_{Ca} is Ca^{2+} channel conductance. Rather, I_{Ca} has a nonlinear dependence on the Ca^{2+} driving force (McCormick and Huguenard 1992). That relationship is well described by the Goldman-Hodgkin-Katz (GHK) equation, $I_{Ca} = a(\exp(zq(V\text{-}E_{Ca})/kT)\text{-}1)/(\exp(zqV/kT)\text{-}1)$, where a is a constant related to Ca^{2+} membrane permeability, z is the ionic valence of a Ca ion, $z = 2$, q is the unit electronic charge, k is the Boltzmann constant and T is the absolute temperature. At room temperature, which was used by Jackson et al. (2004), $kT/2q = 12.5$ mV. The extracellular concentration of Ca^{2+} for the results in Jackson et al. (2004) was 1.2 mmol/L ($Ca_o^{2+} = 1.2$ mmol/L). The level of Ca_i^{2+} in neurons is significantly less than 1.2 mmol/L. At rest, $Ca_i^{2+} = 50$ nmol/L (McCormick and Huguenard 1992). During an AP, Ca_i^{2+} in the immediate vicinity of BK channels may rise to the 10–20 μmol/L range (Fakler and Adelman 2008), which is also considerably less than 1.2 mmol/L. For the purposes of the GHK equation Ca_i^{2+} may assumed to be zero without significantly altering the results in this report over the range of potentials spanned by an AP. For $Ca_i^{2+} = 0$, $I_{Ca} = -\ aGHK(V)$ with $GHK(V) = (V/12.5)/[\exp(V/12.5)\text{-}1]$. Note that $GHK(V = 0) = 1$. For the purposes of BK channel activity as well as other features of SCN neuron behavior, Ca_i^{2+} is, of course, not zero. In particular, Ca_i^{2+} undoubtedly has "hot spots" adjacent to the Ca/BK complexes within the membrane during an AP (Fakler and Adelman 2008). This distribution has been simplified for modeling purposes by the assumption of two intracellular compartments for Ca_i^{2+} (Yamada et al. 1998; Diekman et al. 2013). One compartment corresponds to a thin spherical shell 0.1 μmol/L in thickness near the membrane surface (McCormick and Huguenard 1992). The Ca^{2+} concentration in this compartment is denoted by Ca_s. The other compartment corresponds to the cytosol. The Ca_s parameter is given by:

$$dCa_s/dt = -K_1 I_{Ca} - K_2 Ca_s + c_s \quad (4)$$

with $K_1 = 3 \times 10^{-5}$ M/nC, $K_2 = 0.04$ ms^{-1} (Purvis and Butera 2005), $c_s = 2$ nmol/L/ms, and

$$I_{Ca}(V,t) = -GHK(V)f(t)[305r_1^2(V,t) + 31r_2(V,t)] \quad (5)$$

where $f(t)$ is I_{Ca} inactivation, and r_1 and r_2 are the gating activation parameters for the two types of I_{Ca} channels present in SCN neurons, one of which appears to be the L-type channel based on its sensitivity to nimodipine. The other component is nimodipine-insensitive (Jackson et al. 2004). A full description of the I_{Ca} model is given in Clay (2015). The model was previously applied to the AP in the inset of Figure 5B of Jackson et al. (2004) - Fig 8 of Clay (2015) - used for their AP-clamp recording of I_{Ca}. A similar analysis was carried out here (Fig. 2, bottom panel) for the AP illustrated in Figures 1 and 2 which, as

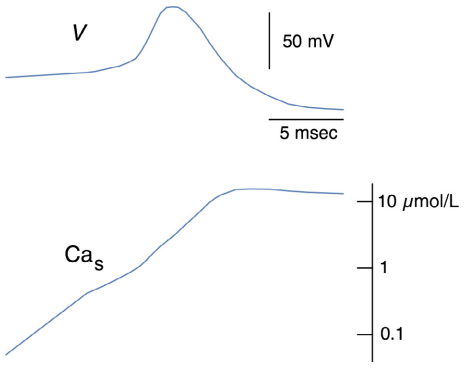

Figure 2. Top panel: Same AP is in Figure 1. Bottom panel: Calcium ion concentration adjacent to the internal surface of the membrane, referred to here as Ca_s, obtained using the AP in the top panel, as described in the text.

noted above, corresponds to the AP used by Jackson et al. (2004) for their AP-clamp recording of I_{BK}. The I_{Ca} analysis must necessarily be carried out for the *same* AP used for the AP-clamp recording of I_{BK}.

I_{BK} model

The model for I_{BK}, Equations 1–3, predicts a response to a rectangular voltage clamp step that is consistent with a single exponential function of time, as in the results of Cui et al. (1997). Similar results have been reported for BK splice variants heterologously expressed in HEK cells (Shelley et al. 2013), as well as results from *mslo*/CaV channel complexes also heterogously expressed in HEK cells (Cox 2014). As noted above, the Ca_s dependence of the model is contained in the V_{Ca}, α_{Ca}, and β_{Ca} parameters. Specifically, $V_{Ca} = 147–75\ Log[Ca_s/Ca_o]$ mV with $Ca_o = 1\ \mu$mol/L, $\alpha_{Ca} = 0.03/[1 + (Log\{Ca_s/Ca_o\})^2]$, and $\beta_{Ca} = 0.04/[1 + (Log\{Ca_s/Ca_o\})^2]$. The predictions of the model for voltage steps from 20 to 110 mV in 10 mV increments with $Ca_s = 10.2\ \mu$mol/L are shown in the left-hand panel of Figure 3. These results are to be compared with the corresponding experimental recordings in Figure 1A of Cui et al. (1997). The deactivation kinetics in the right-hand panel of Figure 3 are to be compared with the corresponding results in Figure 1B of Cui et al. (1997).

Ca_i^{2+} dependence of I_{BK} results

Cui et al. (1997) reported results for $Ca_i^{2+} = 0.84$, 1.7, 4.6, and 10.2 μmol/L, as well as higher levels of Ca_i^{2+}. The channel activation curves for $0.84 \le Ca_i^{2+} \le 10.2\ \mu$mol/L, given in their Figure 5B, are reproduced here in Figure 4. These results represent currents at the end of 20 msec duration voltage steps, sufficiently long so that the channel kinetics at any given voltage were at their steady-state level. In the model these results correspond to $n_\infty = \alpha_{BK}(V,V_{Ca})/(\alpha_{BK}(V,V_{Ca})+\beta_{BK}(V,V_{Ca}))$ with α_{BK} and β_{BK} as given by Equation 3. The predictions of this equation for n_∞ are represented by the curves in Figure 4. The time constants of the model, τ_{BK}, are given by $\tau_{BK} = 1/(\alpha_{BK}+\beta_{BK})$. This equation predicts the bell-shaped curves in Figure 5 shown along with experimental results for τ_{BK} from Cui et al. (1997) corresponding to $Ca_i^{2+} = 0.84$, 1.7, and 10.2 μmol/L. The curve for $Ca_s = 0.84\ \mu$mol/L is shifted leftward on the voltage axis by an increase in Ca_s similar to the results for the activation curves (Figure 4). The maximal time constant at any given level of Ca_s is itself dependent upon Ca_s, a bell-shaped dependence as indicated in Figure 1D of Cox (2014). Results for τ_{BK} from Cui et al. (1997) and Cox (2014) normalized by the maximum time constant for $Ca_i^{2+} = 0.9\ \mu$mol/L in the Cox (2014) report are shown in Figure 6 along with the corresponding prediction of the model, $1/[1 + (Log\{Ca_s/Ca_o\})^2]$. Cox (2014) reported results for $Ca_i^{2+} = 0.003\ \mu$mol/L and 118 μmol/L (neither of which is shown in Figure 6). The former is below the resting level of Ca_i^{2+}, which is 0.05 μmol/L (McCormick and Huguenard 1992). The latter, $Ca_i^{2+} = 118\ \mu$mol/L, would appear to be well above the maximum level of Ca_i^{2+} reached during an AP (10–20 μmol/L, Berkenfeld et al. 2006; Fakler and Adelman 2008). Cox (2014) described a detailed model of BK channel activation including the effects of Ca_i^{2+} on activation gating. The model in this report is relatively simple, which is useful for the analysis of I_{BK} during an AP. Those results are qualitatively similar to the experimental recording of I_{BK}, although their timing does not completely match experiment. The simulations assume that the effect of a change in Ca_s on BK

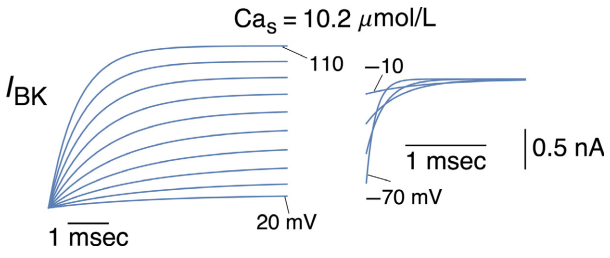

Figure 3. Predictions of the model in Equations 1–3 for I_{BK}. Left panel: Currents elicited from the model with 6 msec duration voltage clamp steps from +20 to +110 mV, with 10 mV increments between each step. Initial value of $n(t)$ in Equation 2 at the beginning of each step was $n = 0$. Right panel: Deactivation currents for an initial value of $n = 1$ with $V = -10$, -30, -50, and -70 mV.

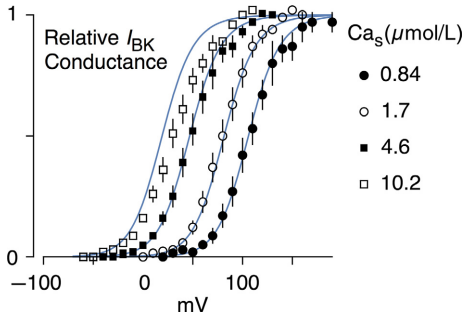

Figure 4. Relative conduction for I_{BK} as a function of Ca_s. The data points with error bars were taken from Figure 5B from Cui et al. (1997). The curves correspond to $n_\infty = \alpha_{BK}/(\alpha_{BK} + \beta_{BK})$ with α_{BK} and β_{BK} given in Equation 3 and $\alpha_{Ca} = 0.03/[1 + (Log\{Ca_s/Ca_o\})^2]$, $\beta_{Ca} = 0.04/[1 + (Log\{Ca_s/Ca_o\})^2]$, and $V_{Ca} = 147–75\ log[Ca_s/Ca_o]$ mV.

channel kinetics occurs instantaneously. Alternatively, a delay of a few milliseconds may be involved (Hille 2001; Martinez-Espinosa et al. 2014), which could account for the difference between experiment and theory in Figure 1.

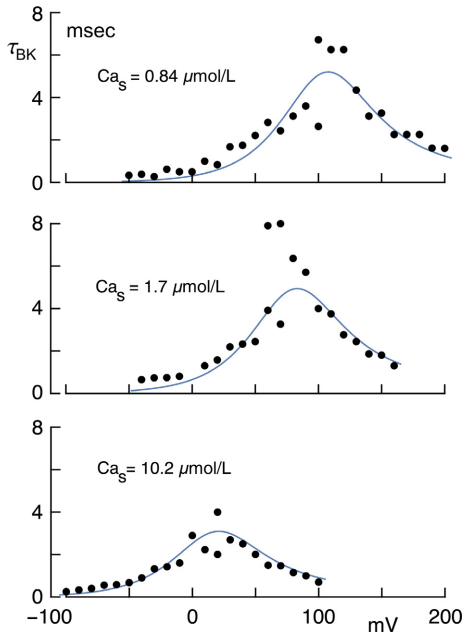

Figure 5. Time constants of I_{BK} for three different levels of Ca_s. The data points are from Cui et al. (1997). Specifically, the results for Ca_s = 0.84, 1.7, and 10.2 μmol/L were taken from Figure 2A and 3A, 2B and 3B, and 2C and 3C, respectively (Cui et al. 1997), the right-hand panel in each case. The lines correspond to $\tau_{BK} = 1/[\alpha_{BK}(V) + \beta_{BK}(V)]$ with $\alpha_{BK}(V)$ and $\beta_{BK}(V)$ as given in Equation 3 in the text.

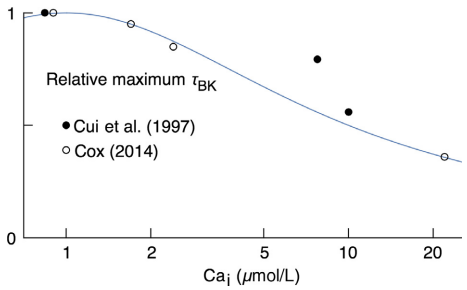

Figure 6. Relative maximum time constants as a function of Ca_i^{2+} (Ca_s) from Cui et al. (1997) and Cox (2014). The results for Cui et al. (1997) correspond to the maximum values of the curves in Figure 5: Ca_s = 0.84 μmol/L, 5.3 msec; Ca_s = 1.7 μmol/L, 5.0 msec; Ca_s = 10.2 μmol/L, 3.1 msec. The results from Cox (2014) were taken from Figure 1D of that report: Ca_s = 0.9 μmol/L, 5.8 msec; Ca_s = 2.4 μmol/L, 4.2 msec; Ca_s = 7.8 μmol/L, 1.9 msec, and Ca_s = 22 μmol/L, 1.5 msec. These results were normalized relative to the Ca_s = 0.9 μmol/L result from Cox (2014). The curve corresponds to $1/[1 + (\text{Log}\{Ca_s/Ca_o\})^2]$ with Ca_o = 1 μmol/L.

Discussion

As noted above (Introduction), Whitt et al. (2016) have suggested that BK channel inactivation is a significant factor in SCN excitability. Specifically, BK_i, the primary BK channel component during the day, exhibits pronounced inactivation during voltage clamp step recordings, whereas BK_s, the primary BK component at night, does not. However, significant inactivation of BK occurs only for $V > +30$ mV (Whitt et al. 2016; Fig. 2a), which is above the maximum overshoot potential of the SCN AP (Jackson et al. 2004; Fig. 2). Moreover, the time constant of inactivation at potentials for which it does occurs is ~45 msec, and that result is relatively insensitive to changes in V (Whitt et al. 2016). The duration of the SCN AP at its midpoint is ~4 msec (Jackson et al. 2004), significantly less than the time constant of inactivation. The membrane potential spends considerably less time than 4 msec at potentials greater than 0 mV. These observations taken together suggest that BK inactivation is not an important factor for excitability in the SCN. Another aspect of BK channel gating, its activation curve, could be significant. The β2 subunit not only produces inactivation of BK at strongly depolarized potentials, it also shifts the BK channel activation curve leftward on the voltage axis for a given level of Ca_i^{2+} (Wallner et al. 1999; Xia et al. 1999). Results from BK_i and BK_s channels in rat adrenal chromaffin cells (RCC) may be relevant to the roles of these channels in the SCN. The activation curve for BK_i in those cells is also shifted leftward relative to the activation curve for BK_s (Sun et al. 2009). Constant current injection in a model of an RCC with BK_i produces repetitive firing, whereas constant current injection in model cell having BK_s produces only one or a very few APs (Sun et al. 2009). As noted by Sun et al. (2009), "...These differences arise, not because of the inactivation behavior of BK_i current, but from the more negatively shifted range of activation of BK_i channels at a given Ca_i^{2+} in comparison to BK_s current." A similar conclusion may apply to the SCN. Specifically, the diurnal changes that occur in the SCN may be attributable to a voltage shift of the BK channel activation curve produced by the β2 subunit rather than inactivation of the BK channel which, additionally, appears to occur outside of the range of membrane potentials spanned by an AP. The results in this report are based on a clone of the α subunit, a BK channel which does not possess the β2 subunit. A leftward shift of the activation curve attributable to that subunit may produce an increase in the difference between experiment and theory in Figure 1, a delay in the onset of the

effects of a change in Ca_s on BK channel gating that is greater than the delay indicated in Figure 1. Additional experiments and simulations of I_{BK} during an AP may be needed to clarify this issue.

The effects of Ca_i^{2+} on BK channels are similar, in some respects, to the effects of Ca_i^{2+} on synaptic vesicle release in nerve terminals following an AP (Neher 1998; Augustine et al. 2003). An AP triggers entry of Ca^{2+} into the terminal via voltage-gated Ca^{2+} channels. These channels almost certainly lie in close proximity to vesicle release sites. As a result, the local Ca^{2+} concentration may briefly rise to levels of 100 μmol/L, or higher (Neher 1998). BK channel activation in presynaptic nerve terminals has been used to report these levels of Ca_i^{2+} (Yazejian et al. 2000). Following an AP, vesicle release drops precipitously, which is consistent with a similarly rapid drop in Ca_i^{2+}, probably due to various Ca^{2+} buffering mechanisms (Parnas and Parnas 1994; Neher 1998). In SCN neurons Ca^{2+} channels are likely to be in close proximity to BK channels similar to the relationship between Ca^{2+} channels and vesicle release sites in presynaptic nerve terminals. During an AP, the Ca^{2+} concentration in the vicinity of BK channels may rise to somewhere in the 10–20 μmol/L range, or perhaps higher (Berkenfeld et al. 2006; Fakler and Adelman 2008). The simulation in Figure 2 is consistent with this result. Specifically, Ca_s equals 15 μmol/L midway through repolarization of the AP. Calcium ion buffers may not be required to reduce this level of Ca_i^{2+} thereby terminating BK channel activation because repolarization of the AP, a process to which I_{BK} contributes, brings the membrane potential below BK channel threshold even with Ca_s in the 1–10 μmol/L range. In this sense I_{BK} is self-limiting. The time between APs in a spontaneously firing SCN neuron during the day is approximately 100 msec, considerably longer at night, either of which is sufficient for Ca^{2+} to diffuse passively away from the membrane bringing Ca_s to its baseline level prior to the subsequent AP. Indeed, Ca_s in the simulation in Figure 2 is reduced below 15 μmol/L by passive diffusion even before the AP has ended.

Voltage-dependent activation of BK channels may not require the presence of Ca_i^{2+}, although strong depolarizations are needed for channel activation with very low Ca_i^{2+}. For example, Cui et al. (1997) reported *mslo* channel currents with Ca_i^{2+} = 0.5 nmol/L. Cox (2014) reported similar results with Ca_i^{2+} = 3 nmol/L. The midpoint of the channel activation curve for these conditions is V = +200 mV for Ca_i^{2+} = 0.5 nmol/L and V = +150 mV for Ca_i^{2+} = 3 nmol/L, both of which are well positive to the range of potentials spanned by an AP even with a 50-60 mV leftward shift of the activation curve on the voltage axis caused by the $\beta 2$ subunit (Xia et al. 1999).

As noted above, this work may have significant implications for computational models of the AP for neurons in which BK channels are present. In traditional models, such as the Hodgkin and Huxley (1952) model of the AP in squid giant axons, the intracellular and extracellular concentrations of permeant ions, Na^+ and K^+ in the case of squid axons, are fixed throughout the AP although the effective extracellular K^+ concentration can change due to K^+ accumulation in the extracellular space between the axolemma and the surrounding Schwann cell (Frankenhauser and Hodgkin 1956). This effect can be accounted for in the AP model by assigning a time dependence to E_K (Clay 1998). The intracellular Ca^{2+} concentration provides another example of an ion concentration not remaining fixed during an AP, especially in the vicinity of BK channels. This result does not significantly change the driving force, V-E_{Ca}, over the range of potentials spanned by the AP (Clay 2015). The intracellular Ca^{2+}concentration, Ca_i^{2+}, does not appear in the expression given above for GHK(V) - RESULTS. A change in Ca_i^{2+} does modify BK kinetics, perhaps with a delay and that delay would have to be accounted for in a model of the AP.

Conflict of Interest

No conflict of interest, financial or otherwise, are declared by the author.

REFERENCES

Augustine, G. J., F. Santamaria, and K. Tanaka. 2003. Local calcium signaling in neurons. Neuron 40:331–346.

Bean, B. P. 2007. The action potential in mammalian central neurons. Nat. Rev. Neurosci. 8:451–465.

Belle, M. D., C. O. Diekman, D. B. Forger, and H. D. Piggins. 2009. Daily electrical silencing in the mammalian circadian clock. Science 326:281–284.

Berkenfeld, H., C. A. Sailer, W. Bildl, V. Rohde, J. O. Thumfart, S. Eble, et al. 2006. BK_{Ca}-Cav channel complexes mediate rapid and localized Ca^{2+}-activated K^+ signaling. Science 314:615–620.

Clay, J. R. 1998. Excitability of the squid giant axon revisited. J. Neurophysiol. 80:903–913.

Clay, J. R. 2015. Novel description of ionic currents recorded with the action potential clamp technique: application to excitatory currents in suprachiasmatic nucleus neurons. J. Neurophysiol. 114:707–716.

Cloues, R. K., and W. A. Sather. 2003. Afterhyperpolarization regulates firing rate in neurons of the suprachiasmatic nucleus. J. Neurosci. 23:1593–1604.

Colwell, C. S. 2006. BK channels and circadian output. Nat. Neurosci. 9:985–986.

Cox, D. H. 2014. Modeling a Ca^{2+} channel/BK_{Ca} channel complex at the single-complex level. Biophys. J . 107:2797–2814.

Cui, J., D. H. Cox, and R. W. Aldrich. 1997. Intrinsic voltage dependence and Ca^{2+} regulation of *mslo* large conductance Ca-activated K^+ channels. J. Gen. Physiol. 109:647–673.

Diekman, C. O., M. D. Belle, R. P. Irwin, A. N. Allen, H. D. Piggins, and D. B. Forger. 2013. Causes and consequences of hyperexcitation in central clock neurons. PLoS Comput. Biol. 9:e1003196.

Fakler, B., and J. P. Adelman. 2008. Control of K_{Ca} channels by calcium nano/microdomains. Neuron 59:873–881.

Frankenhauser, B., and A. L. Hodgkin. 1956. The after-effects of impulses in the giant nerve fibres of *Loligo*. J. Physiol. 160:54–61.

Green, D. J., and R. Gillette. 1982. Circadian rhythm of firing rate recorded from single cells in the rat suprachiasmatic brain slice. Brain Res. 245:198–200.

Groos, G., and J. Hendriks. 1982. Circadian rhythms in electrical discharge of rat suprachiasmatic neurons recorded in vitro. Neurosci. Lett. 34:283–288.

Hille, B. 2001. Ion Channels of Excitable Membranes. (3rd ed.). Sinaur, Sunderland, MA., p. 145-146.

Hodgkin, A. L., and A. F. Huxley. 1952. A quantitative description of membrane current and its application to conduction and excitation in nerve. J. Physiol. 117:500–544.

Inouye, S. T., and H. Kawamura. 1979. Persistence of circadian rhythmicity in a mammalian hypothalamic "island" containing the suprachiasmatic nucleus. Proc. Natl. Acad. Sci. U. S. A. 76:5962–5966.

Jackson, A. C., G. L. Yao, and B. P. Bean. 2004. Mechanism of spontaneous firing in dorsomedial suprachiasmatic nucleus neurons. J. Neurosci. 24:7985–7998.

Kent, J., and A. L. Meredith. 2008. BK channels regulate spontaneous action potential rhythmicity in the suprachiasmatic nucleus. PLoS ONE 3:e3884.

Llinas, R., M. Sugimori, and S. M. Simon. 1982. Transmission by presynaptic spike-like depolarization in the squid giant synapse. Proc. Natl Acad. Sci. USA 79:2514–2419.

Martinez-Espinosa, P. L., C. Yang, V. Gonzalez-Peres, X.-M. Xiao, and C. J. Lingle. 2014. Knockout of BK currents in mouse adrenal chromaffin cells and results in slow-wave burst activity. J. Gen. Physiol. 144:275–295.

McCormick, D. A., and J. R. Huguenard. 1992. A model of the electrophysiological properties of thalamocortical relay neurons. J. Neurophysiol. 68:1384–1400.

Meredith, A. L., S. W. Wiler, B. H. Miller, J. S. Takahashi, A. A. Fodor, N. F. Ruby, et al. 2006. BK calcium-activated potassium channels regulate circadian behavioral rhythms and pacemaker output. Nat. Neurosci. 9:1041–1049.

Montgomery, J. R., and A. L. Meredith. 2012. Genetic activation of BK currents in vivo generates bidirectional effects on neuronal excitability. Proc. Natl Acad. Sci. USA 109:18997–19002.

Montgomery, J. R., J. P. Whitt, B. N. Wright, and A. L. Meredith. 2013. Mis-expression of the BK K^+ channel disrupts suprachiasmatic nucleus circuit rhythmicity and alters clock-controlled behavior. Am. J. Physiol. Cell Physiol. 304:C299–C311.

Neher, E. 1998. Vesicle release pools and Ca^{2+} microdomains: new tools for understanding their roles in neurotransmitter release. Neuron 20:389–399.

Parnas, H., and I. Parnas. 1994. Neurotransmitter release at fast synapses. J. Membr. Biol. 142:267–279.

Pitts, G. R., H. Ohta, and D. G. McMahon. 2006. Daily rhythmicity of large-conductance Ca^{2+}-activated K^+ currents in suprachiasmatic nucleus neurons. Brain Res. 1071:54–62.

Purvis, L. K., and R. J. Butera. 2005. Ionic current model of a hypoglossal motoneuron. J. Neurophysiol. 93:723–733.

Shelley, C., J. P. Whitt, J. R. Montgomery, and A. L. Meredith. 2013. Phosphorylation of a constitutive serine inhibits BK channel variants containing the alternative exon "SKKR". J. Gen. Physiol. 142:585–598.

Shibata, S., Y. Oomura, H. Kita, and K. Hattori. 1982. Circadian rhythmic changes of neuronal activity in the suprachiasmatic nucleus of the rat hypothalamic slice. Brain Res. 247:154–158.

Sun, L., Y. Xiong, X. Zeng, Y. Wu, N. Pan, C. J. Lingle, et al. 2009. Differential regulation of action potentials by inactivating and noninactivating BK channels in rat adrenal chromaffin cells. Biophys. J . 97:1832–1842.

Wallner, M., P. Meera, and L. Toro. 1999. Molecular basis of fast inactivation in voltage and Ca^{2+}-activated K+ channels: a transmembrane beta-subunit homolog. Proc. Natl Acad. Sci. USA 96:4137–4142.

Whitt, J. P., J. R. Montgomery, and A. L. Meredith. 2016. BK channel inactivation gates daytime excitability in the circadian clock. Nat. Comm. 7:10837.

Xia, X. M., J. P. Ding, and C. J. Lingle. 1999. Molecular basis for the inactivation of Ca^{2+}- and voltage-dependent BK channels in adrenal chromaffin cells and rat insulinoma tumor cells. J. Neurosci. 19:5255–5264.

Yamada, W., C. Koch, and P. Adams. 1998. Multiple channels and calcium dynamics. Pp. 137–170 in C. Koch, I. Segev, eds. Methods in Neuronal Modeling, From Synapses to Networks (2nd ed.). MIT Press, Cambridge, MA.

Yamazaki, S., M. C. Kerbeshian, C. G. Hocker, G. D. Block, and M. Mekaker. 1998. Rhythmic properties of the hamster suprachiasmatic nucleus in vivo. J. Neurosci. 18:10709–10723.

Yazejian, B., X.-P. Sun, and A. D. Grinnell. 2000. Tracking presynaptic Ca^{2+} dynamics during neurotransmitter release with Ca^{2+}-activated K^+ channels. Nat. Neurosci. 3:566–571.